

Exploring Transferability of Multimodal Adversarial Samples for Vision-Language Pre-training Models with Contrastive Learning

Youze Wang, Wenbo Hu, Yinpeng Dong, Hanwang Zhang, Hang Su, Richang Hong, *Member, IEEE*,

Abstract—The integration of visual and textual data in Vision-Language Pre-training (VLP) models is crucial for enhancing vision-language understanding. However, the adversarial robustness of these models, especially in the alignment of image-text features, has not yet been sufficiently explored. In this paper, we introduce a novel gradient-based multimodal adversarial attack method, underpinned by contrastive learning, to improve the transferability of multimodal adversarial samples in VLP models. This method concurrently generates adversarial texts and images within imperceptible perturbation, employing both image-text and intra-modal contrastive loss. We evaluate the effectiveness of our approach on image-text retrieval and visual entailment tasks, using publicly available datasets in a black-box setting. Extensive experiments indicate a significant advancement over existing single-modal transfer-based adversarial attack methods and current multimodal adversarial attack approaches.

Index Terms—Vision-and-Language Pre-training, Multimodal, Adversarial Attack, Adversarial Transferability.

I. INTRODUCTION

VISION-Language Pre-training (VLP) models are essential for integrating visual and textual data, which is considered as a significant focus of current research aimed at bridging the gap between vision and language understanding [1]–[4]. The contrastive learning effectively aligns cross-modal feature representations by attracting matched image-text pairs and repelling non-matched pairs, demonstrating a profound capacity to learn generalizable and transferable multimodal features without reliance on labeled data [5]. The efficacy of this alignment strategy in VLP models has led to substantial advancements in various applications [1], [2], [5]–[7], notably in image-text retrieval, visual entailment, visual question answering, and visual grounding, showcasing their transformative potential in multimodal understanding.

It is well studied that adversarial robustness can introduce vulnerabilities through minor adversarial perturbations to inputs, whether textual [9], [10], visual [11]–[14] or audio [15]. Based on it, transfer-based adversarial attacks are proposed which are considered more practical in real-world applications [8], [16], [17]. Some preliminary efforts have been

Y. Wang, W. Hu and R. Hong are at the School of Computer Science and Information Engineering, Hefei University of Technology, Hefei 230009, China. (e-mail: {wenbohu, hongrc}@hfut.edu.cn)

Y. Dong and H. Su are at Tsinghua University, Beijing, 100084, China. (e-mail: dongyinpeng@mail.tsinghua.edu.cn, suhangss@tsinghua.edu.cn)

H. Zhang is with the School of Computer Science and Engineering, Nanyang Technological University, Singapore 639798. (e-mail: hanwangzhang@gmail.com)

Corresponding author: Wenbo Hu.

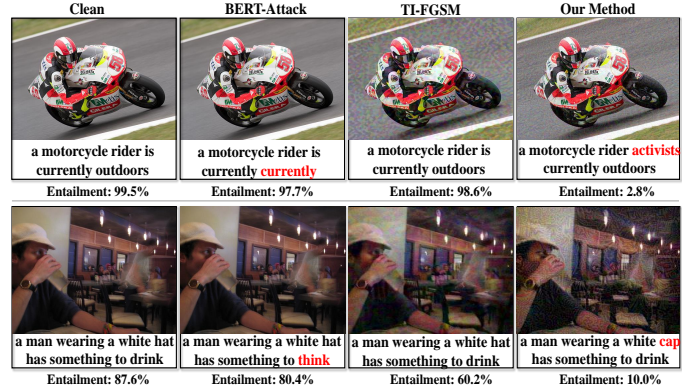


Fig. 1. In a black-box setting, we show three adversarial samples generated by our methods and single-modal adversarial attack methods (TI-FGSM [8] and Bert-Attack [9]). **Top row**: the victim model is TCL [2]. **Bottom row**: the victim model is ALBEF [1]. The probabilities of these adversarial samples by the victim models are also provided below each pair of adversarial samples.

undertaken to explore the adversarial robustness of the VLP models. The co-attack method proposed to give a sequential text-then-image approach to generate multi-modal adversarial samples in a white-box setting [18]. The robustness of the large VLP models is evaluated under the task of image-text generation and considers the transferability in a box-box style. Though comprehensive, this evaluation study is limited to the single-modal adversarial sample, namely image inputs [19]. SGA [20] extends the Co-attack framework by incorporating data augmentation with cross-modal guidance. This enhancement facilitates the transferability of multimodal adversarial samples through sequential optimization.

It is worth noting that currently the adversarial attacks in VLP models lack the intricate interplay between text and image modalities. For effective modality alignments, multimodal adversarial attacks must target each modality individually and meanwhile preserve the contextual integrity of the adversarial pair, as shown in Figure 1. Due to the discrete nature of texts and contrasts sharply with the continuous nature of images, developing a unified framework for generating the transferable adversarial text-image pair represents an unexplored yet critical area of research.

In this paper, we propose a gradient-based multimodal adversarial attack method with contrastive learning (VLP-attack) to generate transferable multimodal adversarial samples against VLP models. Specifically, we combine the textual adversarial attack and visual adversarial attack into a unified

framework based on gradients, which can produce the adversarial texts and the adversarial images simultaneously by gradients under perceptibility constraints. Moreover, we use image-text contrastive loss and intra-modal contrastive loss to improve the transferability of multimodal adversarial samples. We apply the general paradigm in VLP models: CLIP as the surrogate model and prove our method outperforms the existing single-modal transfer-based adversarial attack methods [9], [19], [21]–[23] and multimodal adversarial attack method [18], [20] in the image-text retrieval task and the visual entailment task where the victim models include CLIP series [24], [25], ALBEF [1], TCL [2], BLIP [3], BLIP2 [4], and MiniGPT-4 [26].

In summary, the main contributions are listed as follows:

- Diverging from previous methods, our research employs gradient-based techniques to simultaneously optimize adversarial text and images, investigating transfer-based multimodal adversarial attacks against VLP models.
- To effectively disturb the alignment of image-text representation in a black-box setting, we provide contrastive learning with sufficient image-text variations to perturb the inherent structures in the benign samples and the contextual integrity of image-text pairs from different views.
- We conduct comprehensive experiments and analysis to demonstrate our method outperforms other baselines including single-modal and multimodal adversarial attacks.

II. RELATED WORKS

In this section, we introduce the related works, including visional language pretraining, self-supervised contrastive learning, and black box adversarial attack and its transferability.

A. Vision-Language Pre-training (VLP) and Contrastive Learning

Recent advancements in VLP models have been substantial. These models, trained on extensive datasets of images and corresponding textual descriptions, aim to synthesize understanding between visual and textual data, enhancing vision-language tasks. One such groundbreaking model is CLIP [5], which excels in image-text similarity and zero-shot multimodal tasks, and demonstrates a sophisticated capability to concurrently process and reason about both visual and textual information. ALBEF [1], aligning image and text representations before fusing them with a multimodal encoder, further enhances its learning capabilities from noisy web data through a momentum distillation process. TCL [2] employs triple contrastive learning to harness complementary information from different modalities, thus improving representation learning and alignment. BLIP [3] leverages a dataset bootstrapped from large-scale noisy image-text pairs to pre-train a multimodal encoder-decoder model. Building upon this, BLIP2 [4] introduces a lightweight Querying Transformer to achieve effective vision-language alignment with frozen unimodal models. MiniGPT-4 [26] marks another stride in this field, aligning the visual model with a large language model, making it particularly suitable for image-grounded text generation tasks.

Contrastive learning [5], known for its excellent alignment of text-image features for VLP models, encourages the learned features away from the invariant of augmentations of negative samples, resulting in more generalizable and intrinsic attributes across different models. To enrich the feature space, data augmentation techniques [27]–[29] usually be employed to generate augmentations for image-text pairs. Collectively, these VLP models with contrastive learning underscore the importance of aligning image and text features to enhance performance on various downstream tasks. However, existing transfer-based attacks, primarily focused on single-modal data [8], [19], [23], [30], [31], have been inadequate for more complex tasks requiring a nuanced understanding of multimodal information.

B. Black-box Adversarial Attack and Transferability

Black-box adversarial attacks and their transferability have gained significant attention in recent years due to the vulnerability of machine-learning models to adversarial samples [31]–[34]. Compared with the white-box adversarial attack [11], [35], the black-box attack assuming no knowledge about the target model is a harder setting to study adversarial transferability. In the transfer-based black-box setting, the text adversarial attack methods: Bert-attack [9], PWWS [36], GBDA [21], and image adversarial attack methods: MI-FGSM [22], TI-FGSM [8], SI-NI-FGSM [23], C-GSP [37] and [38], [39], generate adversarial samples on surrogate models at a white-box setting to attack other target models, even when the attacker has no access to the target model’s architecture, gradients, or parameters. However, given the complexity of multimodal data, traditional transfer-based strategies against vision-only models, designed for single-modal data, fall short in effectively perturbing the alignment between text and image features in VLP models. Crafting multimodal adversarial samples with high transferability thus presents a significant challenge.

C. Multimodal Adversarial Attack

While Vision-Language Pretraining (VLP) models have achieved remarkable advancements in various vision-language tasks, the adversarial robustness of these models, particularly the alignment of image and text features, remains unexplored. Zhang’s work [18] delves into adversarial attacks on VLP models in a white-box setting, offering valuable insights for designing multimodal adversarial attacks and enhancing model robustness. Similarly, Wang [35] introduces a white-box adversarial attack specifically targeting multimodal text generation tasks. Zhao [19] investigates the robustness of large VLP models through perturbing the images modality in a black-box setting. Lu [20] enhances the transferability of multimodal adversarial samples by utilizing cross-modal interactions and data augmentation. While white-box attacks provide theoretical understanding, it is the black-box attack—more emblematic of real-world situations—that presents substantial practical security challenges. Addressing this, our study introduces a transfer-based multimodal adversarial attack method. This method is capable of concurrently generating

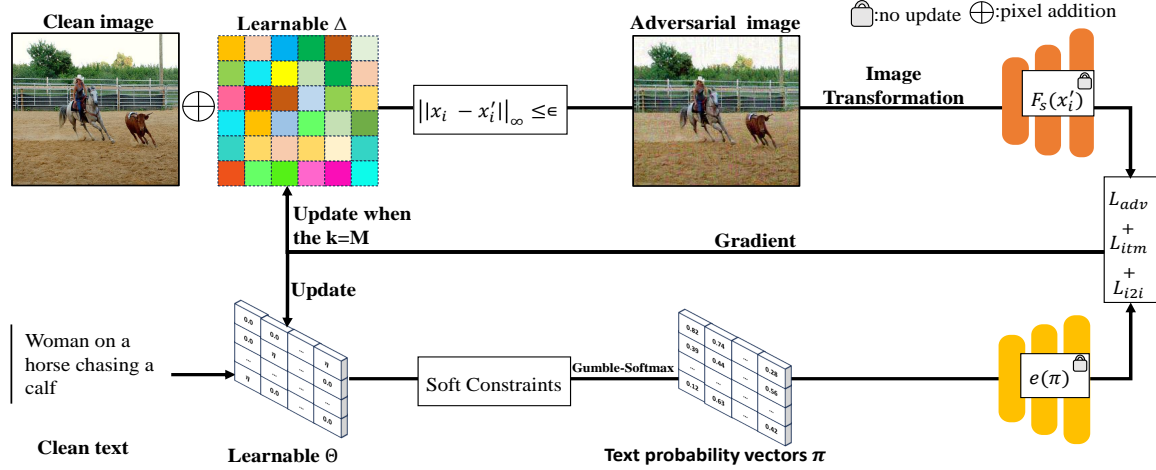


Fig. 2. Illustration of VLP-attack. We propose a multimodal adversarial attack against VLP models, which is based on gradients to generate both adversarial text and adversarial images simultaneously, and leverages image-text contrastive loss and intra-modal contrastive loss to improve the transferability of multimodal adversarial samples. Δ is the perturbation for images and θ is the parameterized matrix for the Gumble-softmax sampling. $e(\cdot)$ is an embedding function. M is the number of image transformations.

both adversarial texts and images with high transferability, thereby enabling a more comprehensive examination of the black-box adversarial perturbations within VLP systems

III. METHODOLOGY

Our proposed method has two contributions: (1) we optimize the perturbation and generate the multimodal adversarial samples simultaneously by unifying them into a gradient-based framework, which can better attack the vulnerable multimodal information that has similar semantics. (2) we use contrastive learning to perturb the inherent structures in the benign samples and the contextual integrity of image-text pairs from various views, which can improve the transferability of the generated multimodal adversarial samples.

A. Problem Formulation

Given an image-text pair, our goal is to minimize the semantic similarity between the image and the corresponding text with minor adversarial perturbations on images and texts on surrogate models. Let x_i denote an original image, x_t denote an original text, x'_i denote an adversarial image, x'_t denote an adversarial text, and y^t denote the corresponding ground-truth label in the image-text retrieval task and the visual entailment task. We use \mathcal{F}_s to denote the surrogate VLP models and \mathcal{F}_v to denote the victim VLP models, where the output of \mathcal{F}_s is the feature representation of the input and the output of \mathcal{F}_v is the prediction score. To generate valid multimodal adversarial samples, we need to minimize the cosine similarity Loss function J :

$$L_{adv} = \begin{cases} \min J(\mathcal{F}_s(x'_i), \mathcal{F}_s(x'_t)) \\ s.t. \|x'_i - x_i\|_\infty \leq \epsilon \\ s.t. \text{similarity}(x'_t, x_t) \leq \beta \end{cases} \quad (1)$$

on surrogate models and make $\mathcal{F}_v((x'_i, x'_t)) = y^{adv}$ ($y^t \neq y^{adv}$) on victim models. For the image x'_i , under the constraint, the adding perturbation should look visually similar to the

benign image x_i . For the text x'_t , we modify the words in a benign text x_t , which can not affect the original semantic understanding for humans. In this work, we use the L_∞ norm to constrain the perceptibility of adversarial perturbations, i.e., $\|x'_i - x_i\|_\infty \leq \epsilon$. For the fluency of x'_t , we constrain the x'_t with the objective of the next token prediction by maximizing the likelihood given previous tokens. For the semantic similarity between x_t and x'_t , we use the bert score to constrain the adversarial text x'_t . The framework of VLP-attack is shown in Figure 2.

B. The objective for multimodal Adversarial Perturbation

The optimization objective of multimodal adversarial perturbation consists of three components: image-text semantic similarity loss L_{adv} for multimodal adversarial sample, soft constraints for adversarial texts, and contrastive loss for transferability, where L_{adv} has been introduced in section 3.1.

1) *Soft Constraints for Adversarial Texts: Adversarial Text Distribution.* Due to the discrete nature of text data, the first step of optimizing both the adversarial texts and the adversarial images simultaneously based on gradients is to transform the text into a continuous distribution. Motivated by [21], we can obtain the text distribution through the Gumble-softmax [40]. Specifically, for a sequence of words $x_t = [w_1, w_2, \dots, w_n]$ where each $w_j \in \mathcal{V}$ and \mathcal{V} is a fixed vocabulary, we use a Gumble-softmax distribution P_θ parameterized by a matrix $\Theta \in \mathbb{R}^{n \times V}$ to sample a sequence of probability vectors π , where $\pi = \pi_1 \dots \pi_n$, and use an embedding function $e(\cdot)$ to convert π to input text embedding. Samples π and adversarial text features $e(\pi)$ are obtained according to the process:

$$(\pi_k)_j := \frac{\exp((\Theta_{k,j} + g_{k,j})/t)}{\sum_{v=1}^V \exp((\Theta_{k,v} + g_{k,v})/t)} \quad (2)$$

$$e(\pi) = e(\pi_1) \cdots e(\pi_n) \quad (3)$$

where $g_{k,j} \sim \text{Gumble}(0,1)$ and $t > 0$ is a temperature parameter that controls the smoothness of Gumble-softmax distribution.

Soft Constraint. For the fluency of the generated adversarial texts, we maximize the likelihood of the next token prediction when giving previous tokens:

$$L_{perp}(\pi) := - \sum_{k=1}^n \log p_{dis}(\pi_k | \pi_1 \cdots \pi_{k-1}) \quad (4)$$

where $\log p_{dis}$ is the cross-entropy between the next word distribution and the previously predicted word distribution. Meanwhile, for the semantic similarity between adversarial texts and origin texts, we use BERT score [41] to constraint the semantic gap:

$$L_{sim}(x_t, x'_t) = \sum_{k=1}^n w_k \max_{j=1, \dots, m} \phi(x_t)_k^\top \phi(x'_t)_j \quad (5)$$

where $x_t = x_{t,1} \cdots x_{t,n}$ and $x'_t = x'_{t,1} \cdots x'_{t,m}$. $\phi(\cdot)$ is a language model that can generate contextualized embeddings for the token sequences.

2) *Contrastive Loss for Transferability:* To improve the transferability of multimodal adversarial samples, we utilize contrastive learning including intra-modal contrastive learning and image-text contrastive learning to push the adversarial samples away from different views of the benign samples. Formally, the infoNCE loss for image-to-text is defined as:

$$L_{nce}(x_i, x_t^+, x_t^-) = E \left[\log \frac{e^{(sim(x_i, x_t^+)/\tau)}}{\sum_{k=1}^K e^{(sim(x_i, \hat{x}_{t,k})/\tau)}} \right] \quad (6)$$

where τ is a temperature hyper-parameter, \hat{x}_t is a set of all positive samples and negative samples for benign image x_i .

Cross-modal contrastive Loss. In image-text contrastive learning, our goal is to minimize the semantic similarity between the adversarial image and adversarial text that is matched in the original space. In image-to-text loss, the original text and text augmentations are taken as negative samples x_t^- . In text-to-image loss, the original image and image augmentations are regarded as negative samples x_i^- . Intuitively, we encourage the features of the adversarial images and benign textual features to be unaligned in the embedding space, which can affect the multimodal features fusion in turn. Taken the image-to-text contrastive loss and text-to-image contrastive loss together as follows:

$$L_{itm} = \frac{1}{2} [L_{nce}(x'_t, x_i^+, x_t^-) + L_{nce}(x'_i, x_t^+, x_i^-)] \quad (7)$$

However, in addition to minimizing the semantic association between the adversarial images and the adversarial texts, we should also focus on the differences between the perturbed information and the original information in images.

Intra-modal Contrastive Loss. we utilize intra-modal contrastive learning to push adversarial samples semantically different from the benign samples in the same modality. Specifically, we consider some random views $(x_{i,1}, x_{i,2}, \dots, x_{i,n})$ of the benign image x_i under random data augmentation as negative samples x_i^- , and randomly sample images from the test set as the positive samples x_i^+ .

$$L_{i2i} = L_{nce}(x'_i, x_i^+, x_i^-) \quad (8)$$

We utilize contrastive learning to discover and attack generalized patterns and structures in multimodal data so that multimodal adversarial samples can avoid trapping into model-specific local optimization making worse transferability of adversarial samples.

Objective Function. We combine all the above losses into a final objective for the gradient-based multimodal adversarial samples generation :

$$L = a \cdot L_{adv} + b \cdot L_{perp} + c \cdot L_{sim} + d \cdot L_{itm} + g \cdot L_{i2i} \quad (9)$$

where a, b, c, d, g are the hyper-parameters that can control the strength of different constraint terms. Our purpose is to maximize the $L(\Theta, x'_i)$ by optimizing the matrix Θ for adversarial text x'_t and the perturbation on the image x'_i .

C. The generation of multimodal adversarial samples

We apply the gradient to optimize the adversarial texts and adversarial images simultaneously. For the adversarial texts, we optimize the matrix Θ as follows:

$$\begin{cases} g_{\Theta}^j = \nabla_{\Theta} L(\mathcal{F}_s(x_i^j), e(\pi^j)) \\ \Theta^{j+1} = f(\Theta^j, \alpha_{\Theta}, g_{\Theta}^j, m_{\Theta}^j) \end{cases} \quad (10)$$

where L is the total loss in eq (9), α_{Θ} is the learning rate for Θ , g_{Θ}^j is the gradient of Θ at iteration j , m_{Θ}^j is the momentum at iteration j , and f is the function of updating the weights of Θ .

For the images that are continuous data, similar to the momentum updating approach in [23], we use a variation of normal gradient descent to make a jump in the direction of previously accumulated gradients before computing the gradients in each iteration. Meanwhile, following the [16], we diverse the pattern of x_i^j . we input (x'_i, x'_t) to \mathcal{F}_s and obtain the gradient of x'_i :

$$\begin{cases} x_i^{nes} = T(x_i^j, p) + g_{x_i^j}^j \\ g_{x_i^j}^{j+1} = \mu \cdot g_{x_i^j}^j + \frac{\nabla_{x_i^j} L(\mathcal{F}_s(x_i^{nes}), e(\pi^j))}{\|\nabla_{x_i^j} L(\mathcal{F}_s(x_i^{nes}), e(\pi^j))\|_1} \\ x_i^{j+1} = \text{Clip}_{x_i}^{\epsilon} \{x_i^j + \alpha_{x_i^j} \cdot \text{sign}(g_{x_i^j}^{j+1})\} \end{cases} \quad (11)$$

where T is the stochastic transformation function with the probability p , $\alpha_{x_i^j}$ is the step size, μ is the decay factor of the momentum term, $g_{x_i^j}^j$ is the accumulated gradient at iteration j , and $\text{Clip}_{x_i}^{\epsilon}$ indicates the resulting adversarial images are clipped within the ϵ -ball of the original image x_i .

Compared with the multimodal attack method based on the step-wise scheme [18], [20], we generate both the adversarial texts and the adversarial images simultaneously based on the gradient, which helps to find and attack the vulnerable multimodal information that has similar semantics. The pseudocode of VLP-attack is outlined in Appendix VI.

IV. EXPERIMENTS

In this section, we conduct a comprehensive evaluation of our proposed attack method across two key tasks: image-text retrieval and visual entailment. The objective is to demonstrate the efficacy of VLP-Attack on seven selected victim models. Additionally, we undertake ablation studies to substantiate the individual components of VLP-Attack and present a visualization of a pair of multimodal adversarial samples.

TABLE I
PERFORMANCE OF TRANSFER-BASED ATTACK FOR IMAGE-TEXT RETRIEVAL TASK ON MSCOCO DATASET AND FLICKR30K DATASET.

Model	Attack	MSCOCO (5K test set)						Flickr30K (1K test set)					
		TR			IR			TR			IR		
		R@1 \uparrow	R@5 \uparrow	R@10 \uparrow	R@1 \uparrow	R@5 \uparrow	R@10 \uparrow	R@1 \uparrow	R@5 \uparrow	R@10 \uparrow	R@1 \uparrow	R@5 \uparrow	R@10 \uparrow
ALBEF	BERT-Attack	15.3	8.9	5.6	19.5	18.1	15.0	7.7	0.7	0.4	17.1	9.9	7.2
	GBDA	14.7	13.0	11.1	11.1	15.7	16.2	6.5	1.6	1.2	14.7	13.2	12.5
	TI-FGSM	22.1	14.4	10.1	15.0	12.3	9.2	10.4	3.3	1.9	14.1	7.2	4.5
	SI-NI-FGSM	26.7	19.8	14.7	20.0	18.2	14.7	22.9	12.0	8.9	24.1	14.9	10.8
	AttackVLM	9.1	5.6	3.5	7.4	5.8	4.2	6.6	1.7	1.0	7.5	3.4	2.1
	Co-attack	26.9	17.5	12.5	27.3	26.4	22.8	20.9	12.3	10.6	18.4	11.4	8.5
	SGA	34.3	26.0	19.4	30.6	29.8	25.7	27.9	12.1	9.2	32.4	21.4	16.4
	VLP-attack	38.7	31.9	26.1	32.0	32.8	29.3	35.2	20.4	15.6	38.9	27.8	22.2
TCL	BERT-Attack	15.5	8.5	5.5	18.6	16.8	13.8	6.7	0.6	0.1	15.6	9.1	6.9
	GBDA	8.1	5.4	4.2	9.0	7.3	6.6	3.2	0.7	0.2	9.6	5.6	3.8
	TI-FGSM	14.2	8.5	5.6	9.4	7.6	5.4	22.9	11.7	7.9	24.7	15.0	10.8
	SI-NI-FGSM	27.6	19.6	15.5	19.8	18.1	15.1	23.0	11.5	7.2	24.7	15.3	11.0
	AttackVLM	12.3	7.8	5.3	9.9	8.4	6.5	12.3	7.8	5.3	9.8	8.4	6.5
	Co-attack	27.4	19.2	14.2	27.7	27.2	23.8	15.5	5.4	1.7	26.4	17.5	13.4
	SGA	34.8	26.9	20.7	28.4	28.9	25.4	30.3	14.2	8.8	34.7	23.2	17.4
	VLP-attack	36.2	29.0	23.7	29.1	29.6	26.1	32.3	17.2	12.2	37.4	26.1	20.2
BLIP	BERT-Attack	29.6	17.3	11.2	27.4	24.2	19.7	17.4	4.0	1.5	24.5	12.6	8.8
	GBDA	12.5	6.2	3.2	13.1	9.9	7.6	17.7	10.6	10.3	26.5	18.2	15.8
	TI-FGSM	24.8	13.5	8.6	17.5	12.6	9.5	30.2	13.5	9.1	27.7	15.5	10.8
	SI-NI-FGSM	35.8	24.2	18.3	27.9	23.9	19.4	30.6	13.6	9.1	27.7	15.5	10.7
	AttackVLM	11.1	6.8	4.3	10.3	8.5	6.7	4.7	0.8	0.5	6.3	2.7	1.8
	Co-attack	40.1	27.6	19.3	35.5	33.2	28.3	26.0	7.7	4.1	31.4	18.7	13.2
	SGA	37.5	28.3	22.3	34.0	33.9	30.2	25.0	10.7	7.6	34.0	20.8	15.6
	VLP-attack	49.0	38.4	29.8	39.2	39.0	34.3	44.7	23.3	15.3	43.6	30.4	23.3
BLIP2	BERT-Attack	15.1	6.9	3.9	18.8	14.7	11.8	4.7	0.7	0.1	13.4	6.9	4.6
	GBDA	5.0	3.9	2.5	5.8	4.1	3.0	3.0	0.9	0.4	8.1	4.3	2.8
	TI-FGSM	5.6	2.5	1.3	4.2	3.2	1.9	3.1	0.2	1.8	3.6	1.2	0.7
	SI-NI-FGSM	12.7	6.5	4.2	9.4	7.4	6.0	6.1	1.2	1.0	7.4	3.3	2.2
	AttackVLM	4.4	2.0	1.1	4.0	2.7	2.1	2.8	0.4	0.2	3.3	1.1	0.8
	Co-attack	19.6	9.7	6.2	20.3	17.8	14.2	6.5	1.5	0.5	17.3	9.6	6.7
	SGA	19.9	10.6	7.2	20.2	17.7	14.6	10.7	2.0	0.8	18.2	9.9	7.1
	VLP-attack	22.0	12.7	8.6	20.9	17.9	14.9	11.5	3.2	2.1	20.5	11.3	8.3

TR means Text Retrieval, IR means Image Retrieval

TABLE II
PERFORMANCE OF TRANSFER-BASED ATTACK FOR VISUAL ENTAILMENT TASK ON SNLI-VE DATASET.

Model Attack \uparrow	BERT-Attack	GBDA	TI-FGSM	SI-NI-FGSM	AttackVLM	Co-attack	SGA	VLP-attack
ALBEF	17.6	20.2	10.5	11.8	2.6	22.1	25.5	28.9
TCL	12.1	15.2	8.7	10.2	1.4	21.8	23.4	27.0
BLIP2	7.2	16.2	9.1	16.9	8.6	9.8	18.4	22.0
MiniGPT-4	2.3	11.4	6.1	4.4	4.6	6.1	12.0	12.9

A. Experimental Settings

Datasets and Downstream Tasks. Following Co-attack [18], we use the test set in MSCOCO [42], Flickr30K [43], SNLI-VE [44] to evaluate the effectiveness of our proposed method at different tasks in a black-box setting, where MSCOCO and Flickr30K are used to evaluate the Text Retrieval (TR) and Image Retrieval (IR) tasks, and SNLI-VE is used to evaluate the Visual Entailment (VE) task. Note that due to the nature of the adversarial attack, we select only the image-text pairs with a label of entailment from the test set of the SNLI-VE dataset for the VE task.

Evaluation Metrics. For evaluation, we report (1) the attack success rate (ASR), which measures the rate of successful adversarial samples. **Similar to Co-attack [18], we define the ASR as the results when the original samples are fed into the target models minus the results when the adversarial samples are fed into the target models.** (2) Semantic

Similarity (Sim.), which is computed between the original and adversarial sentences and is commonly approximated by the universal sentence encoder [45]. (3) Tokens error rate (TER.), which is the proportion of words or characters in a text that have been altered to create an adversarial text, generally, less perturbation results in more semantic consistency. The whole method is implemented by Pytorch [46] and all experiments are conducted in a GeForce RTX A6000 GPU.

Hyperparameters. For a fair comparison, the maximum perturbation ϵ is set to 16/255 among all experiments for the adversarial attack on images. The step size is set to $\epsilon/10$. The number of iterations for all image attacks is 10 except for AttackVLM which is 100 according to the setting in the original paper. For the adversarial attack on texts, the max length of each text is set to 30. The adversarial distribution parameter Θ is optimized using RMSProp [47] with a learning rate of 0.3 and a momentum of 0.6. For the distribution

TABLE III
EVALUATION OF THE PROPOSED METHODS ON CLIP SERIES MODELS ON IMAGE-TEXT RETRIEVAL TASKS.

Model	Attack	MSCOCO (5K test set)						Flickr30K (1K test set)					
		TR			IR			TR			IR		
		R@1 \uparrow	R@5 \uparrow	R@10 \uparrow	R@1 \uparrow	R@5 \uparrow	R@10 \uparrow	R@1 \uparrow	R@5 \uparrow	R@10 \uparrow	R@1 \uparrow	R@5 \uparrow	R@10 \uparrow
Open CLIP -G/14	AttackVLM	9.1	5.6	3.5	7.4	5.8	4.2	6.6	1.7	1.0	7.5	3.4	2.1
	Co-attack	26.6	22.3	18.2	18.8	19.0	17.0	22.8	6.6	2.8	26.1	18.7	13.7
	SGA	27.4	22.4	18.4	19.2	18.8	17.4	24.2	9.9	5.3	27.8	19.1	14.0
	VLP-attack	28.1	22.7	18.9	19.5	20.8	18.4	32.2	16.7	11.4	33.3	24.1	18.1
EVA-02-CLIP bigE-14-plus	AttackVLM	17.9	10.6	7.4	2.4	2.0	1.7	10.3	2.5	2.3	3.7	3.1	2.8
	Co-attack	20.2	17.4	13.6	18.0	18.2	16.6	20.6	4.1	1.7	24.2	17.1	13.1
	SGA	23.6	19.7	15.8	19.3	19.9	18.1	23.1	5.0	2.6	21.7	15.5	11.3
	VLP-attack	29.7	20.6	15.2	21.0	21.6	19.4	27.9	9.5	5.6	23.5	16.0	12.1

TR means Text Retrieval, IR means Image Retrieval

TABLE IV
THE SEMANTIC SIMILARITY (SIM.) AND TOKEN ERROR RATE (TER.) OF ADVERSARIAL TEXTS FOR ALL THE ATTACKS.

Tasks	Datasets	Metrics	Bert-Attack	GBDA	Co-attack	SGA	VLP-attack
Image-text Retrieval	MSCOCO	Sim. \uparrow	89.9	82.5	89.8	90.0	90.1
		TER. \downarrow	12.3	35.6	12.3	12.3	14.3
	Flickr30K	Sim. \uparrow	90.7	84.6	90.7	90.4	90.3
		TER. \downarrow	10.8	33.4	10.8	10.8	14.6
Visual Entailment	SNLI-VE	Sim. \uparrow	85.7	85.6	85.7	85.8	85.1
		TER. \downarrow	18.1	24.1	18.1	18.1	20.9

parameters, Θ is initialized to zero except $\Theta_{j,k} = \eta$ where j denotes the j_{th} word of the benign text, and k denotes the id of the word. In the experiment, we take $\eta = 13$. For the text augmentation, we use the round-trip translation skill to produce diverse texts. The transformation operations T consist of rotation, polarizing, translation, shear, color jittering, and cropping. The number of images transformation is set to 5, and the probability p is 0.6. The number of data augmentation is set to 7. For the image-text retrieval task, $a = 8, b = c = d = g = 1$. For the visual entailment task, $a = 10, b = c = d = g = 1$.

Vision-Language Pre-training Models. Vision-language representation learning largely benefits from image-text alignment through contrastive losses. The VLP models examined in our work are as follows:

- **CLIP** [5] can understand images and texts simultaneously through image-text contrastive learning, which has been a general paradigm to align the image and text representations in latest VLP models. In this work, we utilize CLIP as the surrogate model to craft the black-box attacks to explore the transferability of multimodal adversarial examples for VLP models and take the **ViT-B/16** as the image encoder.
- **Open CLIP-G/14** [24] utilizes the LAION-2B English subset from the LAION-5B collection for training, employing the Open CLIP framework. Compared to OpenAI’s CLIP-B/16, OpenCLIP-G/14 features an expanded parameter set and a larger training dataset.
- **EVA-02-CLIP-bigE-14-plus** [25] integrates advancements in representation learning, optimization, and augmentation, significantly outperforming OpenAI’s CLIP models with equivalent parameter sizes. In comparison to OpenAI’s CLIP-B/16, EVA-02-CLIP-bigE-14-plus benefits from an expanded dataset and increased parameter count, enhancing its performance.
- **ALBEF** [1] aligns the image and text representation by the image-text contrastive loss before Fusing through cross-attention, which demonstrates the effectiveness on various V+L tasks including image-text retrieval, and visual entailment.
- **TCL** [2] proposes triple contrastive learning for VLP by leveraging both cross-modal and intra-modal self-supervision and firstly takes into account local structure information for multi-modality representation.
- **BLIP** [3] utilizes a dataset bootstrapped from large-scale noisy image-text pairs by injecting diverse synthetic captions and removing noisy captions to pre-train a multimodal encoder-decoder model. The image-text contrastive loss is utilized to align the feature space of the visual transformer and text transformer. Due to the absence of fine-tuned models for the SNLI-VE dataset provided by BLIP, we restricted our utilization of the BLIP model solely to the image-text retrieval task.
- **BLIP2** [4] facilitates the extraction of visual representations that resonate most closely with the textual context. Concurrently, through image-text contrastive learning, there is an alignment of text and image representations. For the image-text retrieval task, we use the BLIP2¹ fine-tuned on the MSCOCO dataset. For the visual entailment task, we use the blip2-opt-2.7b².
- **MiniGPT-4** [26] aligns the visual features with a large language model and can be used for image-grounded text generation tasks. In the experiments, we use Vicuna-7B³ for the visual entailment task.

Transfer-based Adversarial Attack Baselines. To demonstrate the effectiveness of our proposed method, in the transfer-

¹LAVIS/projects/blip2 at main · salesforce/LAVIS (github.com)

²Salesforce/blip2-opt-2.7b · Hugging Face

³Vision-CAIR/vicuna-7b at main (huggingface.co)

based attack setting, we select seven attacks as the baseline methods.

- **Bert-attack** [9] generates adversarial texts that can deceive NLP models while maintaining semantic similarity and grammatical correctness through pre-trained masked language models exemplified by BERT.
- **GBDA** [21] incorporates differentiable fluency and semantic similarity constraints to the adversarial loss and generates the adversarial texts by optimizing a parameterized distribution. For a fair comparison, instead of using GBDA to generate adversarial text by querying against the unknown target model, we sampled the adversarial texts directly from the optimized adversarial distribution.
- **TI-FGSM** [8] is an extension of FGSM [11], which improves upon the FGSM by introducing translation invariance to increase the transferability of adversarial examples between different models.
- **SI-NI-FGSM** [23] adapts the Nesterov accelerated gradient method to jump out of the local optimal solution and utilizes the scale-invariant property to improve the transferability of adversarial images.
- **AttackVLM** [19] is a transfer-based adversarial attack that perturbs the images to evaluate the adversarial robustness of large vision-language models. According to the performance of black-box attack against victim models and settings, we select Matching image-image features (MF-ii) in it.
- **Co-attack** [18] is a multimodal adversarial attack against vision-language pre-training models that adopts a step-wise mechanism that first perturbs the discrete inputs (text) and then perturbs the continuous inputs (image) given the text perturbation, which is designed for white-box attack manner.
- **SGA** [20] is a multimodal transfer-based adversarial attack that investigates the adversarial transferability of recent VLP models through modalities interactions and data augmentation.

B. Main Results

The performance of the adversarial samples generated by our proposed method and other baseline methods against VLP models for the image-text retrieval task and the visual entailment task is reported in Table I, Table II, Table III and Table IV. We have several observations:

- Our proposed VLP-attack, consistently exhibits competitive or superior performance compared to other baseline methods in text-image retrieval and visual entailment tasks, except for a slightly lower performance than Co-attack against EVA-02-CLIP-BigE-14-plus in the Flickr30K, as shown in Table III. This demonstrates the effectiveness of the VLP-attack.
- Compared with single-modal transfer attack methods in Table I and Table II, the multimodal adversarial attack method leverages the joint information from multiple modalities (such as images and texts), the attack can exploit the vulnerabilities and inconsistencies across different modalities, making the attack more effective.

Nonetheless, due to Co-attack being designed for a white-box setting, the attack success rate of multimodal adversarial samples is lower than transfer-based image adversarial attack methods when attacking TCL and BLIP in Flickr30K dataset.

- For the BLIP2 model, the performance of VLP-attack seems a bit more modest, particularly for Text Retrieval. However, in Table VIII ⁴, we observe that as the number of iterations increases, VLP-attack generally demonstrates a positive trend in performance, which indicates that VLP-attack may benefit from more iterations, optimizing the adversarial perturbations.
- Compared to SGA, Co-attack and Bert-attack, the VLP-attack has a slightly higher TER and Similarity as shown in Table IV. This suggests that while VLP-attack might introduce more token-level perturbations, it doesn't compromise the overall semantic integrity of the adversarial texts.
- The VLP-attack, as evidenced by the experimental results, stands out as a potent method in the realm of transfer-based multimodal attacks for perturbing the understanding between images and texts in VLP models. It not only showcases impressive performance metrics across different models but also ensures that the generated adversarial samples preserve their semantic content.

C. Ablation Study

TABLE V
EVALUATION OF THE PROPOSED METHODS ON SNLI-VE DATASET FOR VISUAL ENTAILMENT TASK.

SNLI-VE				
Model	Attack	ASR \uparrow	Sim. \uparrow	TER. \downarrow
ALBEF	VLP-attack@i2i+itm	24.5	85.7	20.5
	VLP-attack@i2i	28.1	85.8	20.2
	VLP-attack@itm	25.9	85.6	20.7
	VLP-attack	28.9	85.1	20.9
TCL	VLP-attack@i2i+itm	20.1	85.7	20.5
	VLP-attack@i2i	26.2	85.8	20.2
	VLP-attack@itm	25.0	85.6	20.7
	VLP-attack	27.0	85.1	20.9
BLIP2	VLP-attack@i2i+itm	18.6	85.7	20.5
	VLP-attack@i2i	19.7	85.8	20.2
	VLP-attack@itm	21.1	85.6	20.7
	VLP-attack	22.0	85.1	20.9
MiniGPT-4	VLP-attack@i2i+itm	10.8	85.7	20.5
	VLP-attack@i2i	11.3	85.8	20.2
	VLP-attack@itm	11.4	85.6	20.7
	VLP-attack	12.9	85.1	20.9

1) *Ablation study on contrastive learning*: We conducted ablation experiments to study the impact of contrastive learning on image-text retrieval tasks and visual entailment tasks. To demonstrate the effectiveness of VLP-attack, we compare variants of VLP-attack with respect to the following perspectives: (1) the effect of image-text contrastive learning, (2) the effect of intra-modal contrastive learning. The following VLP-attack variants are designed for comparison.

⁴To avoid the effect of step size, we set the step size α to 0.1 when the number of iterations is between 20-50, and modify the learning rate to ensure the Sim. and TER. rate closed with that when the number of iterations is 10.

TABLE VI
EVALUATION OF THE PROPOSED METHODS ON FLICKR30K DATASET FOR
IMAGE-TEXT RETRIEVAL TASK.

Flickr30k (1K test set)					
Model	Attack	TR* \uparrow	IR* \uparrow	Sim. \uparrow	TER. \downarrow
ALBEF	VLP-attack@i2i+itm	27.6	20.3	90.4	14.4
	VLP-attack@i2i	31.0	32.6	90.5	14.4
	VLP-attack@itm	30.6	33.1	90.5	14.4
	VLP-attack	35.2	38.9	90.3	14.6
TCL	VLP-attack@i2i+itm	14.5	19.6	90.4	14.4
	VLP-attack@i2i	30.1	34.7	90.5	14.4
	VLP-attack@itm	29.4	31.6	90.5	14.4
	VLP-attack	32.3	37.4	90.3	14.6
BLIP	VLP-attack@i2i+itm	28.6	37.2	90.4	14.4
	VLP-attack@i2i	41.8	41.4	90.5	14.4
	VLP-attack@itm	37.4	38.2	90.5	14.4
	VLP-attack	44.7	43.6	90.3	14.6
BLIP2	VLP-attack@i2i+itm	5.5	11.5	90.4	14.4
	VLP-attack@i2i	6.9	14.0	90.5	14.4
	VLP-attack@itm	10.1	18.9	90.5	14.4
	VLP-attack	11.5	20.5	90.3	14.6

* means the attack success rate of R@1 is reported.

TABLE VII
THE FLUENCY AND SIMILARITY EVALUATION OF THE PROPOSED
METHODS AGAINST ALBEF FOR IMAGE-TEXT RETRIEVAL TASK.

Flickr30k (1K test set)					
Attack	TR* \uparrow	IR* \uparrow	Sim. \uparrow	TER. \downarrow	Perp. \downarrow
VLP-attack@sim	36.0	38.9	88.6	14.3	62.3
VLP-attack@perp	33.6	37.5	90.0	14.0	62.5
VLP-attack	35.2	38.9	90.3	14.6	61.6

* means the attack success rate of R@1 is reported.

- VLP-attack@i2i: A variant of VLP-attack with the intra-modal contrastive learning being removed.
- VLP-attack@itm: A variant of VLP-attack with the image-text contrastive learning being removed.
- VLP-attack@i2i+itm: A variant of VLP-attack with the intra-modal contrastive learning and image-text contrastive learning being removed.

The ablation study results are shown in Table V and Table VI. For the image-text retrieval task and visual entailment task, we can have the following observations:

- The attack success rate (ASR) has a significant drop when removing the contrastive learning, but the similarity (Sim.) and tokens error rate (TER.) change a little, which suggests that contrastive learning contributes to the transferability of multimodal adversarial samples.
- Contrastive learning including image-text contrastive learning and intra-modal contrastive learning all have a positive impact on the transferability of adversarial samples, where the reason is that self-supervised contrastive learning forces the perturbation to focus on the inherent structures in the benign samples from different views and ignore irrelevant factors or nuisances.
- A greater drop in ASR for the image-text retrieval task compared to the visual entailment task when removing the contrastive learning from VLP-attack may be due to the perturbation crafted by contrastive learning can have a greater effect on the alignment for image-text pairs, which is more important in image-text retrieval task.

2) *Ablation study on fluency and similarity of adversarial texts:* We conducted ablation experiments to study the impact of similarity constraints and fluency constraints for adversarial texts in Flickr30k dataset for the image-text retrieval task. We use the Perplexity score (Perp.) to evaluate the fluency of adversarial texts, which is computed with the perplexity score of GPT-2 (large). The following VLP-attack variants are designed for comparison:

- VLP-attack@perp: A variant of VLP-attack with the fluency constraint being removed.
- VLP-attack@sim: A variant of VLP-attack with the similarity constraint being removed.

The ablation study results are shown in Table VII. We can observe that the similarity (Sim.) is reduced from 90.3 to 88.6 and Perplexity (Perp.) is increased from 61.6 to 62.3 when removing the similarity constraints from VLP-attack, which suggests that the similarity constraints contribute to the preservation of adversarial texts’ semantics. For the perplexity constraints, the R@1 in text retrieval (TR), R@1 in image retrieval (IR), and Perp. show obvious change when removing perplexity constraints from VLP-attack, indicating the perplexity constraints can improve the attack success rate and fluency of adversarial texts generated by our method.

Ablation experiments were carried out to assess the influence of contrastive learning, similarity constraints, and fluency constraints in VLP-attack. Our findings reveal that each component in VLP-attack significantly contributes to generating effective multimodal adversarial samples.

D. Sensitivity Analysis

To elucidate the influence of data augmentation number and number of image transformations on the VLP-attack, we conducted a comprehensive sensitivity analysis. This analysis, detailed in Appendix VII, provides a deeper insight into the dynamics and efficacy of the proposed VLP-attack.

E. The Flatness of Loss Landscape Visualization

We visualize the flatness of the loss landscape [48] around x'_i on CLIP for VLP-attack(our method), SGA Co-attack, TI-FGSM, and SI-NI-FGSM, which can be found in Appendix VIII.

F. Visualization

To better understand VLP-attack, we provide the Grad-CAM [49] visualization for the multimodal adversarial samples, against ALBEF for the visual entailment task in Figure 3. The heat map from Grad-CAM can show the attention of the target model for the images when making decisions.

Compared the origin image-text pair with the multimodal adversarial samples in Figure 3 for the visual entailment task, we can observe that the prediction score of ALBEF for the “entailment” is reduced from 59.01% to 3.43% when the perturbation is added to the original image-text pair and the perturbation is in an imperceptible constraint.

TABLE VIII
PERFORMANCE OF VLP-ATTACK ATTACK WITH THE DIFFERENT NUMBER OF ITERATIONS AGAINST BLIP2 FOR IMAGE-TEXT RETRIEVAL TASK

Number of Iteration	Flickr30K (1K test set)						Sim.↑	TER.↓
	Text Retrieval			Image Retrieval				
	R@1↑	R@5↑	R@10↑	R@1↑	R@5↑	R@10↑		
10	11.5	3.2	2.0	20.5	11.3	8.2	90.3	14.6
20	19.7	7.2	5.7	25.2	15.3	11.1	91.9	12.3
30	21.5	8.4	5.3	28.9	18.1	13.4	90.3	14.1
40	22.1	10.1	6.5	30.3	18.5	14.1	90.3	14.6
50	25.4	12.7	7.4	31.9	20.9	15.8	89.7	15.5

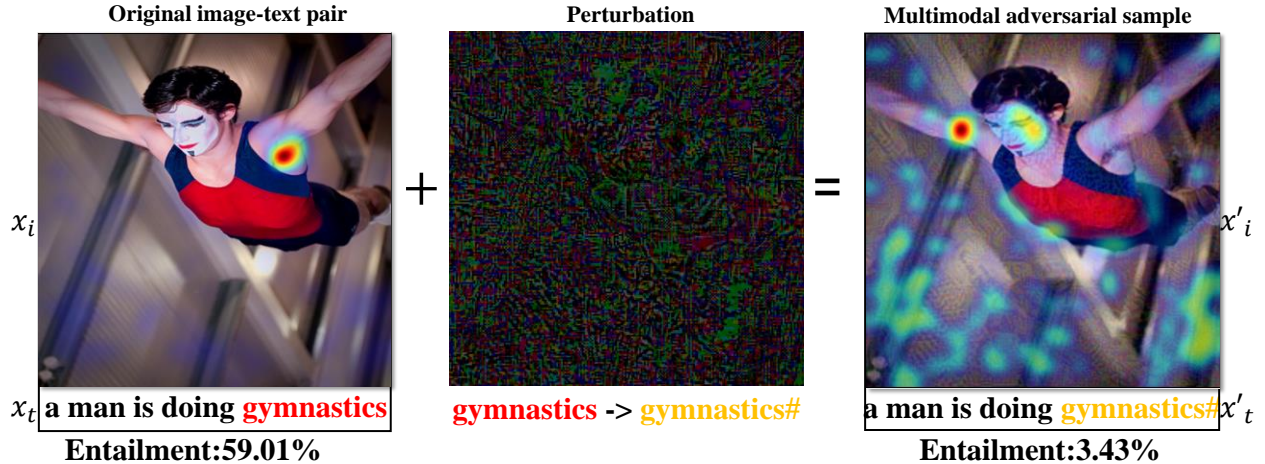


Fig. 3. The Grad-CAM visualizations of the original image-text pair, the multimodal adversarial sample crafted by VLP-attack against ALBEF on SNLI-VE dataset for visual entailment task, where the adversarial perturbation is obtained by $x'_i - x_i$ (pixel values of perturbation are amplified $\times 5$ for visualization).

G. Discussion

We briefly discuss the importance of the work, why contrastive learning can help to generate multimodal adversarial samples with high transferability and the limitations of our work.

The importance of multimodal adversarial attacks. Historically, research on adversarial attacks has concentrated on single-modal data, with multimodal large models primarily studied within white-box attack scenarios. However, multimodal adversarial attacks pose a more significant threat than single-modal attacks, as they can more profoundly affect the models’ ability to interpret and understand visual-language content as shown in Figure 1. As multimodal models play a larger role in the real world, their adversarial robustness is becoming a more pressing issue.

The transferability of contrastive learning. Contrastive learning is used to encourage the adversarial samples away from the semantics of original samples from different views, which benefits to perturb the essential and general characteristics of the samples rather than overfitting to model-specific features on surrogate models as show in Figure 6. This robustness is crucial for transferring adversarial samples to different victim models.

Limitations. Contrastive learning significantly depends on data augmentation to generate positive and negative samples. Ineffectively selected negative samples can induce suboptimal feature perturbations, diminishing the transferability of multimodal adversarial samples. Therefore, the efficacy of positive

and negative sample selection is critical in enhancing VLP-attack transferability, presenting a notable challenge in this domain.

V. CONCLUSION

This paper first proposes a gradient-based multimodal adversarial attack against VLP models in a black-box setting. Compared with the single-modal adversarial attack methods, our method can generate both adversarial text and adversarial images simultaneously, and leverages image-text contrastive loss and intra-modal contrastive loss to improve the transferability of multimodal adversarial samples. The experimental results show that our method outperforms other baselines in image-text retrieval tasks and visual entailment tasks.

REFERENCES

- [1] J. Li, R. Selvaraju, A. Gotmare, S. Joty, C. Xiong, and S. C. H. Hoi, “Align before fuse: Vision and language representation learning with momentum distillation,” *Advances in neural information processing systems*, vol. 34, pp. 9694–9705, 2021.
- [2] J. Yang, J. Duan, S. Tran, Y. Xu, S. Chanda, L. Chen, B. Zeng, T. Chilimbi, and J. Huang, “Vision-language pre-training with triple contrastive learning,” in *Proceedings of the IEEE/CVF Conference on Computer Vision and Pattern Recognition*, 2022, pp. 15 671–15 680.
- [3] J. Li, D. Li, C. Xiong, and S. Hoi, “Blip: Bootstrapping language-image pre-training for unified vision-language understanding and generation,” in *International Conference on Machine Learning*. PMLR, 2022, pp. 12 888–12 900.
- [4] J. Li, D. Li, S. Savarese, and S. Hoi, “Blip-2: Bootstrapping language-image pre-training with frozen image encoders and large language models,” *arXiv preprint arXiv:2301.12597*, 2023.

- [5] A. Radford, J. W. Kim, C. Hallacy, A. Ramesh, G. Goh, S. Agarwal, G. Sastry, A. Askell, P. Mishkin, J. Clark *et al.*, “Learning transferable visual models from natural language supervision,” in *International conference on machine learning*. PMLR, 2021, pp. 8748–8763.
- [6] Z. Gan, Y.-C. Chen, L. Li, C. Zhu, Y. Cheng, and J. Liu, “Large-scale adversarial training for vision-and-language representation learning,” *Advances in Neural Information Processing Systems*, vol. 33, pp. 6616–6628, 2020.
- [7] Y.-C. Chen, L. Li, L. Yu, A. El Kholi, F. Ahmed, Z. Gan, Y. Cheng, and J. Liu, “Uniter: Universal image-text representation learning,” in *European conference on computer vision*. Springer-Verlag, 2020, pp. 104–120.
- [8] Y. Dong, T. Pang, H. Su, and J. Zhu, “Evading defenses to transferable adversarial examples by translation-invariant attacks,” in *Proceedings of the IEEE/CVF Conference on Computer Vision and Pattern Recognition*, 2019, pp. 4312–4321.
- [9] L. Li, R. Ma, Q. Guo, X. Xue, and X. Qiu, “Bert-attack: Adversarial attack against bert using bert,” *arXiv preprint arXiv:2004.09984*, 2020.
- [10] J. Li, S. Ji, T. Du, B. Li, and T. Wang, “Textbugger: Generating adversarial text against real-world applications,” *arXiv preprint arXiv:1812.05271*, 2018.
- [11] I. J. Goodfellow, J. Shlens, and C. Szegedy, “Explaining and harnessing adversarial examples,” *arXiv preprint arXiv:1412.6572*, 2014.
- [12] A. Madry, A. Makelov, L. Schmidt, D. Tsipras, and A. Vladu, “Towards deep learning models resistant to adversarial attacks,” *arXiv preprint arXiv:1706.06083*, 2017.
- [13] H. Yuan, Q. Chu, F. Zhu, R. Zhao, B. Liu, and N. Yu, “Automa: Towards automatic model augmentation for transferable adversarial attacks,” *IEEE Transactions on Multimedia*, vol. 25, pp. 203–213, 2021.
- [14] X. Wei and S. Zhao, “Boosting adversarial transferability with learnable patch-wise masks,” *IEEE Transactions on Multimedia*, 2023.
- [15] X. Du and C.-M. Pun, “Robust audio patch attacks using physical sample simulation and adversarial patch noise generation,” *IEEE Transactions on Multimedia*, vol. 24, pp. 4381–4393, 2021.
- [16] C. Xie, Z. Zhang, Y. Zhou, S. Bai, J. Wang, Z. Ren, and A. L. Yuille, “Improving transferability of adversarial examples with input diversity,” in *Proceedings of the IEEE/CVF Conference on Computer Vision and Pattern Recognition*, 2019, pp. 2730–2739.
- [17] M. Naseer, S. Khan, M. Hayat, F. S. Khan, and F. Porikli, “On generating transferable targeted perturbations,” in *Proceedings of the IEEE/CVF International Conference on Computer Vision*, 2021, pp. 7708–7717.
- [18] J. Zhang, Q. Yi, and J. Sang, “Towards adversarial attack on vision-language pre-training models,” in *Proceedings of the 30th ACM International Conference on Multimedia*, 2022, pp. 5005–5013.
- [19] Y. Zhao, T. Pang, C. Du, X. Yang, C. Li, N.-M. Cheung, and M. Lin, “On evaluating adversarial robustness of large vision-language models,” *arXiv preprint arXiv:2305.16934*, 2023.
- [20] D. Lu, Z. Wang, T. Wang, W. Guan, H. Gao, and F. Zheng, “Set-level guidance attack: Boosting adversarial transferability of vision-language pre-training models,” in *Proceedings of the IEEE/CVF International Conference on Computer Vision*, 2023, pp. 102–111.
- [21] C. Guo, A. Sablayrolles, H. Jégou, and D. Kiela, “Gradient-based adversarial attacks against text transformers,” *arXiv preprint arXiv:2104.13733*, 2021.
- [22] Y. Dong, F. Liao, T. Pang, H. Su, J. Zhu, X. Hu, and J. Li, “Boosting adversarial attacks with momentum,” in *Proceedings of the IEEE conference on computer vision and pattern recognition*, 2018, pp. 9185–9193.
- [23] J. Lin, C. Song, K. He, L. Wang, and J. E. Hopcroft, “Nesterov accelerated gradient and scale invariance for adversarial attacks,” *arXiv preprint arXiv:1908.06281*, 2019.
- [24] G. Ilharco, M. Wortsman, R. Wightman, C. Gordon, N. Carlini, R. Taori, A. Dave, V. Shankar, H. Namkoong, J. Miller, H. Hajishirzi, A. Farhadi, and L. Schmidt, “Openclip,” Jul. 2021, if you use this software, please cite it as below. [Online]. Available: <https://doi.org/10.5281/zenodo.5143773>
- [25] Q. Sun, Y. Fang, L. Wu, X. Wang, and Y. Cao, “Eva-clip: Improved training techniques for clip at scale,” *arXiv preprint arXiv:2303.15389*, 2023.
- [26] D. Zhu, J. Chen, X. Shen, X. Li, and M. Elhoseiny, “Minigt-4: Enhancing vision-language understanding with advanced large language models,” *arXiv preprint arXiv:2304.10592*, 2023.
- [27] Z. Wu, S. Wang, J. Gu, M. Khabsa, F. Sun, and H. Ma, “Clear: Contrastive learning for sentence representation,” *arXiv preprint arXiv:2012.15466*, 2020.
- [28] Y. Meng, C. Xiong, P. Bajaj, P. Bennett, J. Han, X. Song *et al.*, “Cocollm: Correcting and contrasting text sequences for language model pre-training,” *Advances in Neural Information Processing Systems*, vol. 34, pp. 23 102–23 114, 2021.
- [29] M. Bayer, M.-A. Kaufhold, and C. Reuter, “A survey on data augmentation for text classification,” *ACM Computing Surveys*, vol. 55, no. 7, pp. 1–39, 2022.
- [30] X. Wang and K. He, “Enhancing the transferability of adversarial attacks through variance tuning,” in *Proceedings of the IEEE/CVF Conference on Computer Vision and Pattern Recognition*, 2021, pp. 1924–1933.
- [31] Z. Wang, H. Guo, Z. Zhang, W. Liu, Z. Qin, and K. Ren, “Feature importance-aware transferable adversarial attacks,” in *Proceedings of the IEEE/CVF international conference on computer vision*, 2021, pp. 7639–7648.
- [32] Y. Zhu, Y. Chen, X. Li, K. Chen, Y. He, X. Tian, B. Zheng, Y. Chen, and Q. Huang, “Toward understanding and boosting adversarial transferability from a distribution perspective,” *IEEE Transactions on Image Processing*, vol. 31, pp. 6487–6501, 2022.
- [33] S. Sadriyadeh, L. Dolamic, and P. Frossard, “Transfool: An adversarial attack against neural machine translation models,” *arXiv preprint arXiv:2302.00944*, 2023.
- [34] Y. Dong, S. Cheng, T. Pang, H. Su, and J. Zhu, “Query-efficient black-box adversarial attacks guided by a transfer-based prior,” *IEEE Transactions on Pattern Analysis and Machine Intelligence*, vol. 44, no. 12, pp. 9536–9548, 2021.
- [35] Y. Wang, W. Hu, and R. Hong, “Iterative adversarial attack on image-guided story ending generation,” *IEEE Transactions on Multimedia*, 2023.
- [36] D. Jin, Z. Jin, J. T. Zhou, and P. Szolovits, “Is bert really robust? a strong baseline for natural language attack on text classification and entailment,” in *Proceedings of the AAAI conference on artificial intelligence*, vol. 34, no. 05, 2020, pp. 8018–8025.
- [37] X. Yang, Y. Dong, T. Pang, H. Su, and J. Zhu, “Boosting transferability of targeted adversarial examples via hierarchical generative networks,” in *Computer Vision—ECCV 2022: 17th European Conference, Tel Aviv, Israel, October 23–27, 2022, Proceedings, Part IV*. Springer, 2022, pp. 725–742.
- [38] C. Li, S. Gao, C. Deng, W. Liu, and H. Huang, “Adversarial attack on deep cross-modal hamming retrieval,” in *Proceedings of the IEEE/CVF International Conference on Computer Vision*, 2021, pp. 2218–2227.
- [39] L. Gao, Z. Huang, J. Song, Y. Yang, and H. T. Shen, “Push & pull: Transferable adversarial examples with attentive attack,” *IEEE Transactions on Multimedia*, vol. 24, pp. 2329–2338, 2021.
- [40] E. Jang, S. Gu, and B. Poole, “Categorical reparameterization with gumbel-softmax,” *arXiv preprint arXiv:1611.01144*, 2016.
- [41] T. Zhang, V. Kishore, F. Wu, K. Q. Weinberger, and Y. Artzi, “Bertscore: Evaluating text generation with bert,” *arXiv preprint arXiv:1904.09675*, 2019.
- [42] T.-Y. Lin, M. Maire, S. Belongie, J. Hays, P. Perona, D. Ramanan, P. Dollár, and C. L. Zitnick, “Microsoft coco: Common objects in context,” in *Computer Vision—ECCV 2014: 13th European Conference, Zurich, Switzerland, September 6–12, 2014, Proceedings, Part V 13*. Springer, 2014, pp. 740–755.
- [43] B. A. Plummer, L. Wang, C. M. Cervantes, J. C. Caicedo, J. Hockenmaier, and S. Lazebnik, “Flickr30k entities: Collecting region-to-phrase correspondences for richer image-to-sentence models,” in *Proceedings of the IEEE international conference on computer vision*, 2015, pp. 2641–2649.
- [44] N. Xie, F. Lai, D. Doran, and A. Kadav, “Visual entailment: A novel task for fine-grained image understanding,” *arXiv preprint arXiv:1901.06706*, 2019.
- [45] Y. Yang, D. Cer, A. Ahmad, M. Guo, J. Law, N. Constant, G. H. Abrego, S. Yuan, C. Tar, Y.-H. Sung *et al.*, “Multilingual universal sentence encoder for semantic retrieval,” *arXiv preprint arXiv:1907.04307*, 2019.
- [46] A. Paszke, S. Gross, F. Massa, A. Lerer, J. Bradbury, G. Chanan, T. Killeen, Z. Lin, N. Gimelshein, L. Antiga *et al.*, “Pytorch: An imperative style, high-performance deep learning library,” *Advances in neural information processing systems*, vol. 32, 2019.
- [47] M. D. Zeiler, “Adadelata: an adaptive learning rate method,” *arXiv preprint arXiv:1212.5701*, 2012.
- [48] Z. Qin, Y. Fan, Y. Liu, L. Shen, Y. Zhang, J. Wang, and B. Wu, “Boosting the transferability of adversarial attacks with reverse adversarial perturbation,” *arXiv preprint arXiv:2210.05968*, 2022.
- [49] R. R. Selvaraju, M. Cogswell, A. Das, R. Vedantam, D. Parikh, and D. Batra, “Grad-cam: Visual explanations from deep networks via gradient-based localization,” in *Proceedings of the IEEE international conference on computer vision*, 2017, pp. 618–626.

SUPPLEMENTARY MATERIAL :
EXPLORING TRANSFERABILITY OF MULTIMODAL ADVERSARIAL SAMPLES FOR VISION-LANGUAGE PRE-TRAINING
MODELS WITH CONTRASTIVE LEARNING

VI. THE PSEUDOCODE OF VLP-ATTACK ALGORITHM

VLP-attack optimizes the perturbation and generates the multimodal adversarial samples simultaneously by unifying them into a gradient-based framework, which benefits to destroy the alignment of image-text pairs. In addition, we use a contrastive learning mechanism to perturb the inherent structures in the benign samples and the contextual integrity of image-text pairs from various views to improve the transferability of multimodal adversarial samples, all of which is outlined in Algorithm 1.

Algorithm 1 Transfer-based Multimodal Adversarial Attack

Input: A surrogate model \mathcal{F}_s ; a benign sample $X = \{x_i, x_t\}$, and ground-truth label y ; the size of perturbation ϵ ; learning rate r ; iterations H ; the number of images transformation M ; the probability p of images transformation;

Output: A multimodal adversarial sample $X' = \{x'_i, x'_t\}$;

- 1: Initialize the matrix Θ by x_t , which is used to sample adversarial texts;
- 2: $\alpha_i = \epsilon/H$; $\alpha_\Theta = r$; $x'_i = x_i$; $m_\Theta = \gamma$;
- 3: Generate the images augmentation and texts augmentation;
- 4: **for** $t = 0$ in $H - 1$ **do**
- 5: $g_{x'_i} = 0$
- 6: **for** $k = 0$ in M **do**
- 7: Input (x_i, x_t) to \mathcal{F}_s and calculate the total loss L according to eq (9);
- 8: Obtain the gradient of x'_i : $\nabla_{x'_i} L(\mathcal{F}_s(T(x'_i, p)), x'_t)$;
- 9: Obtain the gradient of Θ : $\nabla_{\Theta} L(\mathcal{F}_s(T(x'_i, p)), x'_t)$;
- 10: Sum the gradients as $g_{x'_i} = g_{x'_i} + \nabla_{x'_i} L(\mathcal{F}_s(T(x'_i, p)), x'_t)$
- 11: Update the weights of matrix Θ according to eq (10);
- 12: **end for**
- 13: Average the gradients of x'_i : $g_{x'_i} = \frac{1}{M} \cdot g_{x'_i}$;
- 14: Update the perturbation δ on x_i according to eq (11);
- 15: **end for**
- 16: Sampling an π from the distribution P_Θ ;
- 17: Obtain the tokens ids in the adversarial text x'_t : $\text{argmax}(\pi)$;
- 18: Obtain the adversarial image x'_i : $x'_i = x_i + \delta$;
- 19: **return** (x'_i, x'_t) ;

VII. SENSITIVITY ANALYSIS

We conducted a comprehensive sensitivity analysis to elucidate the influence of data augmentation number and the number of image transformations on the VLP-attack.

1) *Impact of Data Augmentation Number:* To verify the effect of different data augmentation numbers in VLP-attack, we vary the number of data augmentation from 1 to 9 to craft the multimodal adversarial samples and attack ALBEF

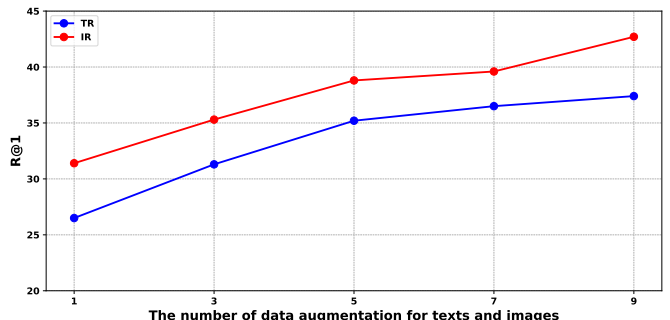


Fig. 4. Effect of data augmentation number. The horizontal coordinate indicates the number of data augmentation and the vertical coordinate indicates the success rate of the attack at R@1 for the image-text retrieval task in Flickr30K dataset.

on Flickr30k dataset for the image-text retrieval task. From Figure 4, we can observe that the attack success rate in R@1 of TR and IR increases with more data augmentation. However, the rate of increase in attack success rates is gradually slowing down, suggesting that on the one hand, adding more augmentation data does not lead to significant performance gains, and on the other hand, VLP-attack may require more fine-grained augmentation data. To balance the cost time and attack success rate, we set data augmentation numbers = 7 in VLP-attack.

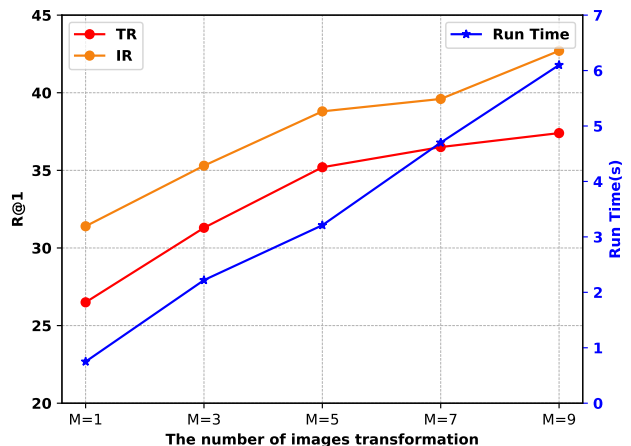


Fig. 5. Effect of images transformation number. The horizontal coordinate indicates the number of images transformation and the left vertical coordinate indicates the success rate of the attack at R@1 for the image-text retrieval task in Flickr30K dataset. The right vertical coordinate indicates the average runtime of different image transformation numbers in VLP-attack when attacking on every image-text pair. The runtime is in seconds.

2) *Impact of Images Transformation Number:* We pad the images with a given probability as the diverse input to improve the transferability of adversarial images. To analyze the effect

of image transformation numbers in VLP-attack, we vary the number of images transformation from 1 to 9 to generate the multimodal adversarial samples in the test set of the Flickr30k dataset. The results of attacking ALBEF using the above adversarial samples are shown in Figure 5. We can observe that R@1 in TR and IR increases with more image transformation numbers, and runtime is gradually increasing due to more image transformations. To balance the cost time and attack success rate, we set image transformation numbers = 5 in VLP-attack.

VIII. THE FLATNESS OF LOSS LANDSCAPE VISUALIZATION

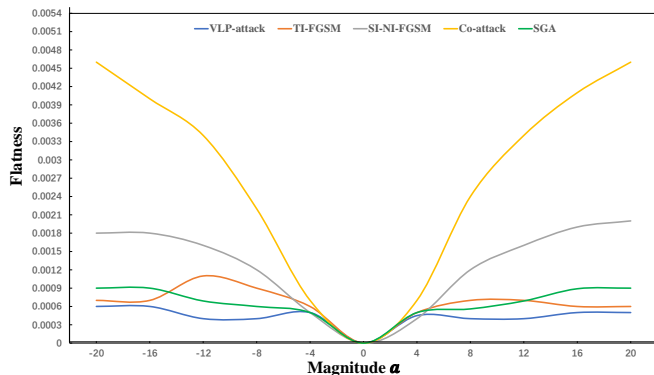


Fig. 6. The flatness visualization of adversarial samples in visual entailment task.

We visualize the flatness of the loss landscape [48] around x'_i on CLIP for VLP-attack(our method), Co-attack, TI-FGSM, and SI-NI-FGSM by plotting the loss change when moving x'_i along a random direction with various magnitudes in the visual entailment task. Specifically, firstly, we sample p from a Gaussian distribution and normalize p on a l_2 unit norm ball, $p \leftarrow \frac{p}{\|p\|_F}$. Then we use different magnitudes a to calculate the loss change(flatness) $f(a)$. The formula is as follows:

$$f(a) = \text{Sim}(\mathcal{F}_s(x'_i + a \cdot p), \mathcal{F}_s(x'_i)) - \text{Sim}(\mathcal{F}_s(x'_i), \mathcal{F}_s(x'_i)) \quad (12)$$

where Sim denotes the function for similarity measurement. Due to the p being randomly sampled, we calculate 20 times with different p and average the value to visualize the flatness of the loss landscape around x'_i .

From Fig 6, we can observe that compared to the baselines, the adversarial images crafted by VLP-attack are located at a much flatter region, which reflects that our method can discover highly robust adversarial examples that exhibit minimal sensitivity to variations in the decision boundary. This effectively reduces the potential overfitting of the surrogate model and improves the transferability of adversarial samples compared with other baselines.